Decreased expression of *TXNIP* is associated with poor prognosis and immune infiltration in kidney renal clear cell carcinoma

WANLU LIU[1], ZHEN XIAO[1], MINGYOU DONG[2], XIAOLEI LI[3] and ZHONGSHI HUANG[1]

[1]School of Basic Medical Sciences, Youjiang Medical University for Nationalities; [2]The Key Laboratory of Molecular Pathology of Hepatobiliary Diseases of Guangxi, Affiliated Hospital of Youjiang Medical University for Nationalities; [3]Scientific Experiment Center, Affiliated Southwest Hospital of Youjiang Medical University for Nationalities, Baise, Guangxi 533000, P.R. China

Received August 7, 2023; Accepted November 16, 2023

DOI: 10.3892/ol.2024.14230

Abstract. The most prevalent and insidious type of kidney cancer is kidney clear cell carcinoma (KIRC). Thioredoxin-interacting protein (*TXNIP*) encodes a thioredoxin-binding protein involved in cellular energy metabolism, redox homeostasis, apoptosis induction and inflammatory responses. However, the relationship between *TXNIP*, immune infiltration and its prognostic value in KIRC remains unclear. Thus, the present study evaluated the potential for TXNIP as a prognostic marker in patients with KIRC. Data from The Cancer Genome Atlas were used to assess relative mRNA expression levels of *TXNIP* in different types of cancer. The protein expression levels of TXNIP were evaluated using the Human Protein Atlas. Enrichment analysis of genes co-expressed with *TXNIP* was performed to assess relevant biological processes that *TXNIP* may be involved in. CIBERSORT was used to predict the infiltration of 21 tumor-infiltrating immune cells (TIICs). Univariate and multivariate Cox regression analyses were used to assess the relationship between *TXNIP* expression and prognosis. Single-cell RNA-sequencing datasets were used to evaluate the mRNA expression levels of *TXNIP* in certain immune cells in KIRC. The CellMiner database was used to analyze the relationship between *TXNIP* mRNA expression and drug sensitivity in KIRC. The results from the present study demonstrated that *TXNIP* expression was significantly decreased in KIRC tissue compared with that in normal tissue, as confirmed by western blotting and reverse transcription-quantitative PCR. In addition, downregulated *TXNIP* expression was significantly associated with poor prognosis, a high histological grade and an advanced stage. The Cell Counting Kit-8 assay demonstrated that *TXNIP* overexpression significantly suppressed tumor cell proliferation. Univariate and multivariate Cox regression analyses indicated that *TXNIP* served as a separate prognostic factor in KIRC. Moreover, *TXNIP* expression was significantly correlated with the accumulation of several TIICs and its overexpression significantly downregulated the mRNA expression levels of CD25 and cytotoxic T-lymphocyte-associated protein 4, immune cell surface markers in $CD4^+$ T lymphocytes. In conclusion, *TXNIP* may be used as a possible biomarker to assess unfavorable prognostic outcomes and identify immunotherapy targets in KIRC.

Correspondence to: Professor Xiaolei Li, Scientific Experiment Center, Affiliated Southwest Hospital of Youjiang Medical University for Nationalities, 8 Chengxiang Road, Baise, Guangxi 533000, P.R. China
E-mail: xiaoleili2004@163.com

Professor Zhongshi Huang, School of Basic Medical Sciences, Youjiang Medical University for Nationalities, 98 Chengxiang Road, Baise, Guangxi 533000, P.R. China
E-mail: zhongshihuang@ymun.edu.cn

Abbreviations: ACC, adrenocortical carcinoma; BLCA, bladder urothelial carcinoma; BRCA, breast invasive carcinoma; CESC, cervical squamous cell carcinoma and endocervical adenocarcinoma; CHOL, cholangiocarcinoma; COAD, colon adenocarcinoma; DLBC, lymphoid neoplasm diffuse large B-cell lymphoma; ESCA, esophageal carcinoma; GBM, glioblastoma multiforme; HNSC, head and neck squamous cell carcinoma; KICH, kidney chromophobe; KIRC, kidney renal clear cell carcinoma; KIRP, kidney renal papillary cell carcinoma; LAML, acute myeloid leukemia; LGG, brain lower grade glioma; LIHC, liver hepatocellular carcinoma; LUAD, lung adenocarcinoma; LUSC, lung squamous cell carcinoma; MESO, mesothelioma; OV, ovarian serous cystadenocarcinoma; PAAD, pancreatic adenocarcinoma; PCPG, pheochromocytoma and paraganglioma; PRAD, prostate adenocarcinoma; READ, rectum adenocarcinoma; SARC, sarcoma; SKCM, skin cutaneous melanoma; STAD, stomach adenocarcinoma; TGCT, testicular germ cell tumor; THCA, thyroid carcinoma; THYM, thymoma; UCEC, uterine corpus endometrial carcinoma; UCS, uterine carcinosarcoma; UVM, uveal melanoma

Key words: TXNIP, KIRC, immune infiltration, prognosis, $CD4^+$ T cell

Introduction

The global incidence of kidney cancer is increasing year by year, and it is highly invasive and metastatic. The most common type of kidney cancer is kidney renal clear cell carcinoma (KIRC) (1,2). Surgery remains the first choice for early treatment due to the fact that KIRC is insensitive to

conventional radiotherapy and chemotherapy (3); however, the disease has an insidious onset, progresses rapidly and is poorly treated with late-stage surgery, resulting in an extremely low late-stage survival rate (4,5). Despite the promising results of targeted therapies (6), the issue of resistance to targeted therapies has arisen. For example, Chatterjee and Bivona (7) found that reversible proteomic and epigenetic mechanisms, tumor microenvironment-mediated mechanisms, and tumor heterogeneity may all contribute to the emergence of resistance, thereby affecting the therapeutic efficacy of cancer treatment.

The use of immunotherapy in cancer has provided novel ideas for the treatment of KIRC, which exhibits a stronger immune response compared with other cancers (8-12). Immunotherapy is effective in prolonging the overall survival (OS) of patients and tumor, node and metastasis (TNM) staging is considered to be the most appropriate prognostic indicator (13-21). However, there are few studies on KIRC immune infiltration and its biomarkers (22). Hence, the search for specific immune biomarkers holds great clinical significance to provide more personalized and precise treatments to improve the prognosis of patients with KIRC.

Thioredoxin-interacting protein (TXNIP), a multifunctional protein that inhibits the production of glucose transporter proteins, enzymes involved in glycolysis and associated genes, is crucial in preventing tumor aerobic glycolysis (23-25). *TXNIP* is associated with the cell cycle process and its upregulation inhibits the function of the cell cycle protein A promoter, thereby suppressing the cell cycle (26). Under oxidative stress, TXNIP in the nucleus is transported to the mitochondria, where it binds to thioredoxin-2, which in turn triggers apoptosis and inhibits the proliferation of tumor cells (27,28). Additionally, *TXNIP* is closely associated with inflammatory immune responses, in which TXNIP binds to the nucleotide-binding oligomerization domain-like receptor family pyrin domain containing 3 inflammasome to induce inflammation (29). Although there are many studies on *TXNIP*, information on immune infiltration and clinical prognosis is scarce (30). Previous studies have reported the relationship between *TXNIP* and angiogenesis, as well as clinical prognosis in KIRC (31,32); however, the relationship between the expression level of *TXNIP* and immune infiltration in KIRC has rarely been reported (33).

In the present study, the mRNA expression level of *TXNIP* in patients with KIRC were assessed using The Cancer Genome Atlas (TCGA) database to evaluate the association with overall survival and clinicopathological characteristics. Additionally, the correlation between *TXNIP* expression level, immune cell infiltration and prognosis was assessed using CIBERSORT and univariate and multivariate Cox regression analysis.

Materials and methods

Data gathering. Using the TCGA database (https://portal.gdc.cancer.gov/), gene expression patterns and clinical information from 542 patients with KIRC and 72 normal kidney tissue samples were obtained from the TCGA-KIRC dataset (34). The Tumor Immune Estimation Resource (TIMER) database was used to determine the mRNA expression levels of *TXNIP* in 33 different cancer types (https://cistrome.shinyapps.io/timer/). The Human Protein Atlas (HPA) database (http://www.proteinatlas.org) was used to obtain immunohistochemical data on protein expression of TXNIP in KIRC and normal tissues.

Identification and enrichment analysis of genes co-expressed with TXNIP. A total of five genes co-expressed with *TXNIP* were screened, with P<0.001 used as a significant correlation cutoff. Gene Ontology (GO) and Kyoto Encyclopedia of Genes and Genomes (KEGG) analyses of co-expressed genes were performed using the R package clusterProfiler v4.6.2. with P<0.05 considered the significance cutoff (35,36). The files 'c2.cp.kegg.v7.4.symbols' and 'c5.go.v7.4.symbols' were used for gene set variation analysis (GSVA). The 'limma' R package v3.54.2 was used to identify biological functions (https://bioinf.wehi.edu.au/limma/). A GSVA score t-value >2 was considered significantly altered.

Evaluation of immune infiltration. The proportion of infiltrating immune cells in 542 tumor samples was assessed using the CIBERSORT database (http://cibersort.stanford.edu/), and the CIBERSORT R v1.03 and LM22 R software packages were used as tools for algorithmic ensembles (37). Based on the median *TXNIP* mRNA expression level of the patients with KIRC, the patients were divided into *TXNIP* low and high expression groups (P<0.05 was considered as a statistically significant screening condition), and the level of infiltration of the different immune cells was subsequently confirmed using the TIMER 2.0 algorithm (38).

Immune checkpoint correlation. A significant correlation of P<0.001 was used as a screening condition and the R package 'corrplot' v0.92 (https://github.com/taiyun/corrplot) was used to assess the correlation between the expression data of immune checkpoint-related genes and *TXNIP* mRNA expression.

Expression levels of TXNIP at the single cell level. The Tumor Immune Single-Cell Hub (http://tisch.comp-genomics.org/home/) is a publicly available and comprehensive web resource site. The KIRC_GSE139555 and KIRC_GSE111360 datasets were selected in the 'Datasets' module to visualize and assess the variations in *TXNIP* expression at the single-cell level between different immune cells.

Drug susceptibility analysis. Drug-related data were obtained from the CellMiner database (39), which includes records of drug sensitivity analysis of drugs validated by clinical trials and approved by the U.S. Food and Drug Administration. Subsequently, Pearson correlation coefficients were used to analyze the relationship between mRNA expression levels of *TXNIP* and drug sensitivity in the TCGA-KIRC dataset.

Cell culture and transfection. Human kidney cancer A498 cells (cat. no. CL-0254) and normal kidney tissue HK-2 cells (cat. no. CM-0109) were obtained from Procell Life Science & Technology Co., Ltd. The cells were resuscitated and cultured with complete minimal essential medium, including MEM basal medium (cat. no. PM150410; Life Science & Technology Co., Ltd.), 1% penicillin mixture (cat. no. P1400; Beijing Solarbio Science & Technology Co., Ltd.), and 10%

neonatal fetal bovine serum [cat. no. CF-01P-02; Cell-Box (HK) Biological products Trading Co., Ltd.]. The cell cultures were kept at 37˚C in a 5% CO_2 cell incubator. Before transfection, the cells were cultured and cultivated until they reached ~70% confluence. A498 cells were then transfected with 4 μg each of *TXNIP*-overexpression plasmid (A498-LV-TXNIP) or empty vector plasmid (A498-LV-Empty). The plasmids were purchased from GeneCopoeia, Inc. The *TXNIP* overexpression and empty vector plasmids were added into MEM basal medium and HighGene plus transfection reagent (cat. no. RM09014P; ABclonal Biotech Co., Ltd.) was then added into the wells containing cells after thorough mixing. After transfection, the cells were placed in a 5% CO_2 cell culture incubator at 37˚C for 4-6 h, and then half of the medium was replaced and the cells were incubated again for 24-48 h before the cells were used for subsequent experiments.

RNA extraction and reverse transcription (RT)-quantitative (q)PCR. An RNA Fast Small Extraction Kit (cat. no. TR154-50; Jianshi Biotechnology Co., Ltd) was used to extract total RNA and cDNA was synthesized using the SureScript™ First-Strand cDNA Synthesis Kit (cat. no. QP056; GeneCopoeia, Inc.). mRNA expression levels were determined using the LightCycler® 96 Instrument (SW 1.1; Roche Diagnostics GmBH) and the BlazeTaq™ SYBR Green qPCR Mix 2.0 kit (cat. no. QP031; GeneCopoeia, Inc.). RNA extraction, cDNA synthesis and qPCR were performed according to the manufacturers' protocols. The synthesis of cDNA was performed at 25˚C for 5 min, 42˚C for 15 min and 85˚C for 5 min, and then annealed at 4˚C to finish. qPCR was performed at 95˚C for 10 min, followed by 40 cycles at 95˚C for 10 sec, 60˚C for 20 sec and extension at 72˚C for 15 sec, with a final extension step at 72˚C for 10 min. GAPDH was used as an endogenous control and the results were quantified using the $2^{-\Delta\Delta Cq}$ method (40). A498 cells (~5x10^5 cells) transfected with empty vector and *TXNIP*-overexpression plasmids were used as control and treatment groups, respectively, and this experiment was repeated three times. The primer sequences (Shanghai Sangon Pharmaceutical Co., Ltd.) used were as follows: GAPDH forward (F), 5'-GGTGAAGGTCGGAGTCAACG-3' and GAPDH reverse (R), 5'-CAAAGTTGTCATGGATGACC-3'; TXNIP F, 5'-GGCAATCATATTATCTCAGGGAC-3' and TXNIP R, 5'-CAGGAACGCTAACATAGATCAGTAA-3'; CD25 F, 5'-TTCGTGGTGGGGCAGATGGT-3' and CD25 R, 5'-TCTTCCCGTGGGTCATTTTG-3'; and cytotoxic T-lymphocyte-associated protein 4 (CTLA4) F, 5'-AACCTACATGATGGGGAATGAG-3' and CTLA4 R, 5'-AGGTAGTATGGCGGTGGGTAC-3'.

Western blotting. Total proteins were extracted from HK-2, A498, A498-LV-TXNIP and A498-LV-Empty cells (~5.5x10^6 cells) using RIPA lysis buffer (Beyotime Institute of Biotechnology) mixed with phenylmethanesulfonyl fluoride (cat. no. P6730; Beijing Solarbio Science & Technology Co., Ltd.) at a ratio of 1:100. The protein concentration was assessed using a BCA protein assay kit (cat. no. PC0020; Beijing Solarbio Science & Technology Co., Ltd.). Subsequently, 70 μg protein/lane were separated on 10% precast gels using SDS-PAGE (Invitrogen; Thermo Fisher Scientific, Inc.) and transferred to PVDF transfer membranes (Biosharp Life Sciences). The membranes were blocked using 5% skim milk powder (cat. no. 1172GR100; BioFroxx; neoFroxx GmbH) for 2 h at room temperature and then incubated with anti-TXNIP (1:1,000; cat. no. A11682; Nature Biosciences Ltd.) and GAPDH antibodies (1:1,000; cat. no. RA0003; Nature Biosciences Ltd.) overnight at 4˚C. The following day, these membranes were washed 3 times using TBST (contains 0.05% Tween) and incubated again with HRP-conjugated goat anti-rabbit IgG (H+L) secondary antibodies (1:3,000; cat. no. AS014; ABclonal Biotech Co., Ltd.) for 1 h at room temperature. Luminescence development was performed using MonPro™ ECL Ultrasensitive Substrate Pro (cat. no. PW30701S; Monad Biotech Co., Ltd.) and a Tanon-5200Multi gel imager was used to capture protein images (Tanon Science and Technology Co., Ltd.). Protein expression levels were semi-quantified using ImageJ v1.8.0 (National Institutes of Health). The GAPDH signal was used to normalize the TXNIP band intensity and the experiment was repeated three times.

Cell Counting Kit (CCK)-8 cell proliferation assay. The CCK-8 was purchased from Dojindo Laboratories, Inc. A498-LV-Empty and A498-LV-TXNIP cells (~2x10^4 cells) were placed in 96-well plates (3x10^3 cells per well) and five wells of each were replicated and cultured in an incubator at 37˚C for 0, 24, 48, 72 and 96 h. CCK-8 reagent (10 μl) was added to each well and then the cells were incubated for another 2 h. Finally, using an ELISA microplate reader [Biobase Biodusty (Shandong) Co., Ltd.], the absorbance values were determined at 450 nm. The experiment was repeated three times.

Statistical analysis. Data handling and statistical analysis was performed using R software version 4.2.1 (https://www.r-project.org/), Strawberry Perl version 5.30.1.1 (https://strawberryperl.com/), SPSS version 25 (IBM Corp.) and GraphPad Prism version 9.0 (Dotmatics). To determine if there were significant differences in *TXNIP*, CD25 and CTLA4 mRNA expression levels between subgroups, analysis was performed using the unpaired t-test. Kruskal-Wallis and Dunn's test were used to analyze the relationship between KIRC clinicopathological variables and *TXNIP* mRNA expression levels. Statistical analysis of Kaplan-Meier and other survival analyses were performed using Log-rank tests. For survival analyses, univariate and multivariate Cox regression models were used. $P<0.05$ was considered to indicate a statistically significant difference.

Results

mRNA expression of TXNIP in certain cancers. The differences in mRNA level expression of *TXNIP* in 33 tumor and normal tissues were compared using data from TCGA database and the TIMER online web tool. TCGA database results showed that the mRNA expression level of *TXNIP* in KIRC was significantly lower than that in normal tissues (Fig. 1A). The 605 samples of KIRC were further evaluated using the TIMER online database, in which the mRNA expression level of *TXNIP* was significantly reduced in 533 tumor samples, which was consistent with the results shown in TCGA database (Fig. 1B). The aforementioned results indicated that *TXNIP* mRNA levels were expressed at a low level in most cancers.

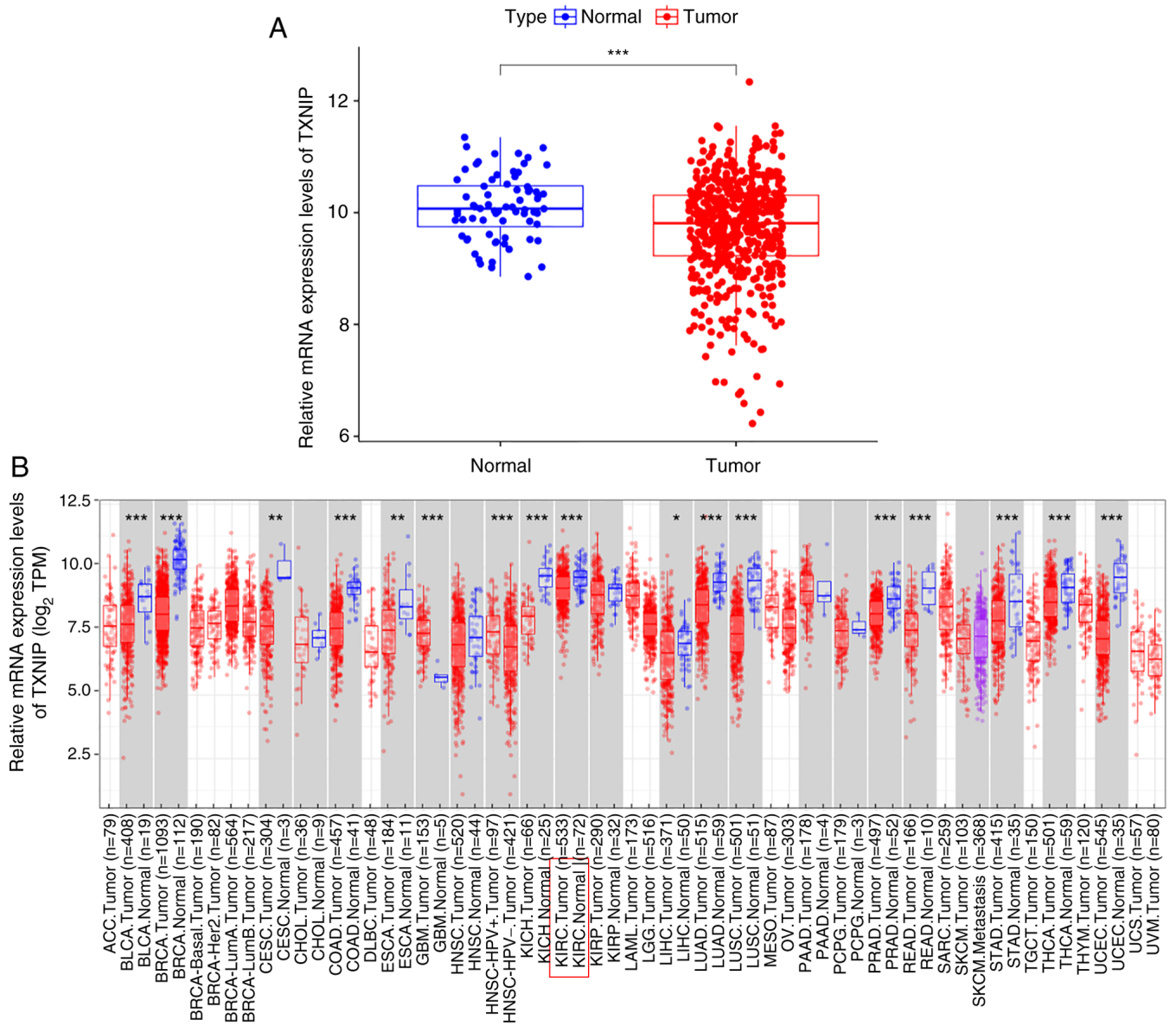

Figure 1. Differential expression of *TXNIP* in different cancers. (A) Differential expression of *TXNIP* in KIRC tumor and normal tissues. (B) Analysis of the differential expression of *TXNIP* in 39 tumors based data from the Tumor Immune Estimation Resource database. *P<0.05, **P<0.01 and ***P<0.001. TXNIP, thioredoxin-interacting protein; KIRC, kidney renal clear cell carcinoma; TPM, transcripts per million; ACC, adrenocortical carcinoma; BLCA, bladder urothelial carcinoma; BRCA, breast invasive carcinoma; CESC, cervical squamous cell carcinoma; CHOL, cholangiocarcinoma; COAD, colon adenocarcinoma; DLBC, lymphoid neoplasm diffuse large B-cell lymphoma; ESCA, esophageal carcinoma; GBM, glioblastoma multiforme; HNSC, head and neck squamous cell carcinoma; KICH, kidney chromophobe; KIRP, kidney renal papillary cell carcinoma; LAML, acute myeloid leukemia; LGG, brain lower grade glioma; LIHC, liver hepatocellular carcinoma; LUAD, lung adenocarcinoma; LUSC, lung squamous cell carcinoma; MESO, mesothelioma; OV, ovarian serous cystadenocarcinoma; PAAD, pancreatic adenocarcinoma; PCPG, pheochromocytoma and paraganglioma; PRAD, prostate adenocarcinoma; READ, rectum adenocarcinoma; SARC, sarcoma; SKCM, skin cutaneous melanoma; STAD, stomach adenocarcinoma; TGCT, testicular germ cell tumors; THCA, thyroid carcinoma; THYM, thymoma; UCEC, uterine corpus endometrial carcinoma; UCS, uterine carcinosarcoma; UVM, uveal melanoma.

Patients with KIRC were matched for clinical data and separated into low and high *TXNIP* expression groups according to their median *TXNIP* mRNA expression level. Kaplan-Meier survival curves and TIMER data (Fig. 2A) demonstrated a positive association between the mRNA expression level of *TXNIP* and cumulative survival. The mRNA expression levels of *TXNIP* in 542 KIRC samples and 72 normal samples were evaluated using TCGA data, and the results showed that KIRC patients with high *TXNIP* expression had significantly improved DSS, OS and progression-free survival (PFS) compared to those with low *TXNIP* mRNA expression levels (Fig. 2B-D). Additionally, the levels of *TXNIP* expression significantly decreased with higher tumor grade, stage and TNM stage (Fig. 2E-I). Thus, it can be seen that the high expression of *TXNIP* could improve the survival rate of patients with KIRC, and that its expression level was negatively associated with the clinicopathological stage.

Protein expression of TXNIP in two types of tissue samples. The TXNIP protein expression level and its clinical significance was assessed using micrographs from patients with KIRC which were included HPA database. TXNIP protein

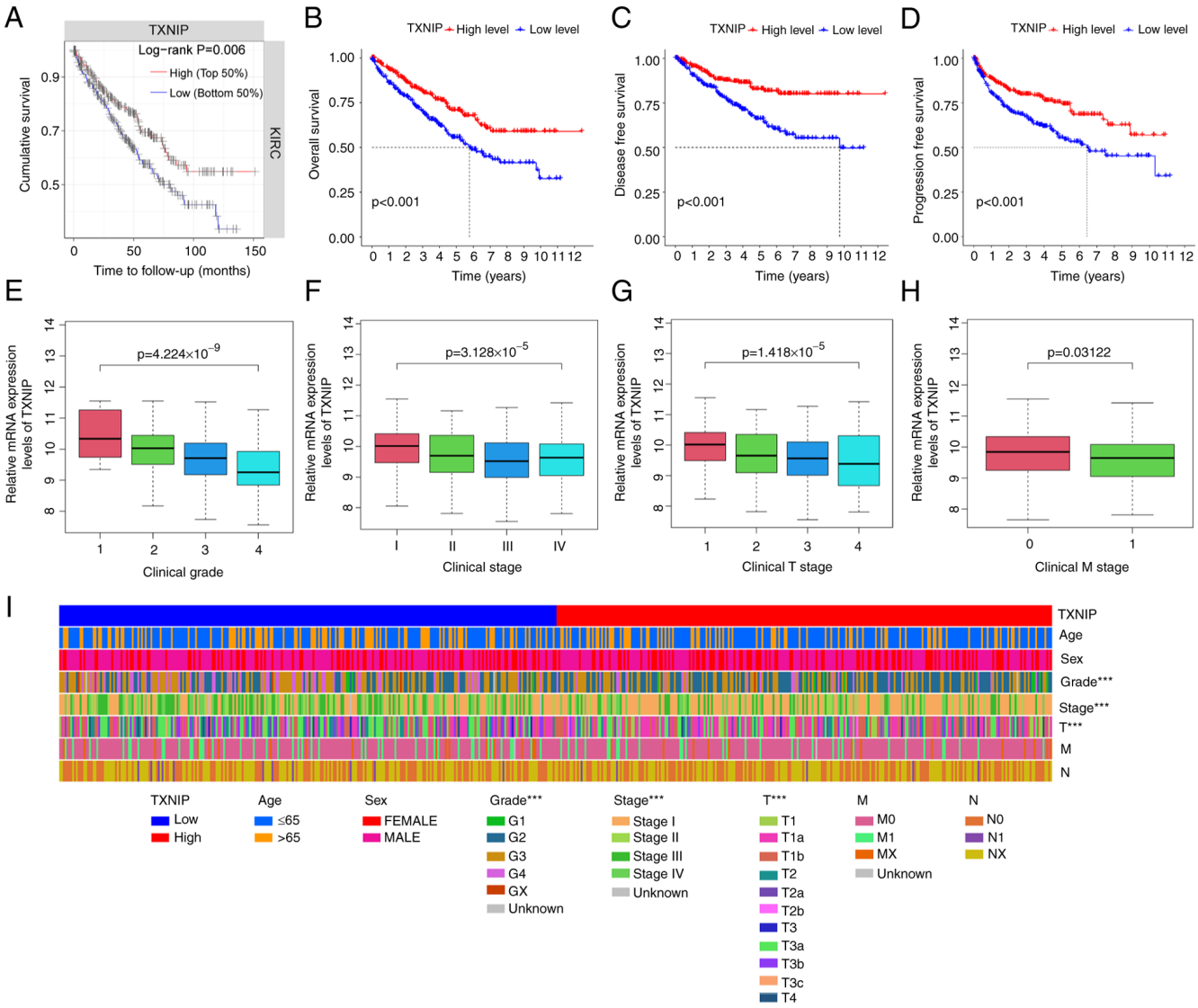

Figure 2. Association between *TXNIP* expression with clinicopathological characteristics of KIRC. (A) Association between OS and the level of *TXNIP* expression using data from the Tumor Immune Estimation Resource database. Reduced expression of *TXNIP* was significantly associated with worse (B) OS, (C) DSS and (D) PFS in patients with KIRC, compared with those with increased expression. *TXNIP* expression significantly decreased with increasing (E) grade, (F) stage, (G) T stage and (H) the occurrence of distant metastases. (I) Relationship between low *TXNIP* expression and age, sex, grade, stage and metastasis. ***P<0.001. TXNIP, thioredoxin-interacting protein; KIRC, kidney renal clear cell carcinoma; OS, overall survival; G, grade; T, tumor; M, metastasis; N, node.

expression was observed to be markedly lower in KIRC tissue samples compared with normal kidney tissue samples, based on immunohistochemistry analysis data from the HPA database (Fig. 3). This result indicates that the protein level of TXNIP in KIRC was also lower than that in normal kidney tissue compared with the mRNA level.

Independent prognostic value of TXNIP in KIRC. Univariate Cox regression analysis demonstrated a significant association between grade and risk scores with OS in 529 patients with KIRC with *TXNIP,* age, grade and stage being statistically significant in KIRC (P<0.001), showing good prognostic value (Fig. 4A). Multivariate Cox regression analysis showed that grade and risk scores were independent prognostic indicators for KIRC, and *TXNIP* had a high prognostic value in KIRC (P=0.012), while age, grade and stage still maintained good prognostic value (P<0.001) (Fig. 4B). Additionally, nomogram plots were constructed that incorporated age, TNM stage, stage, sex and grade to forecast the survival of patients with KIRC at 1, 3 and 5 years, and survival rate was found to decrease significantly with time (Fig. 4C and D). The results suggest that *TXNIP* can be used as an independent prognostic indicator, as well as age, T staging and stage.

TXNIP co-expression analysis. By analyzing 211 genes co-expressed with *TXNIP*, the co-expressed genes were screened using P<0.001 and corFilter=0.7 as threshold conditions (where P<0.001 was an indication of a significant correlation and corFilter=0.7 was used as a criterion for identifying co-expressed genes to filter out irrelevant genes). The results demonstrated that the gene expression of tudor domain containing 7, cold shock domain containing E1, enhancer of polycomb homolog 2, round spermatid basic protein 1 and ribonuclease L had strong and significant positive correlations

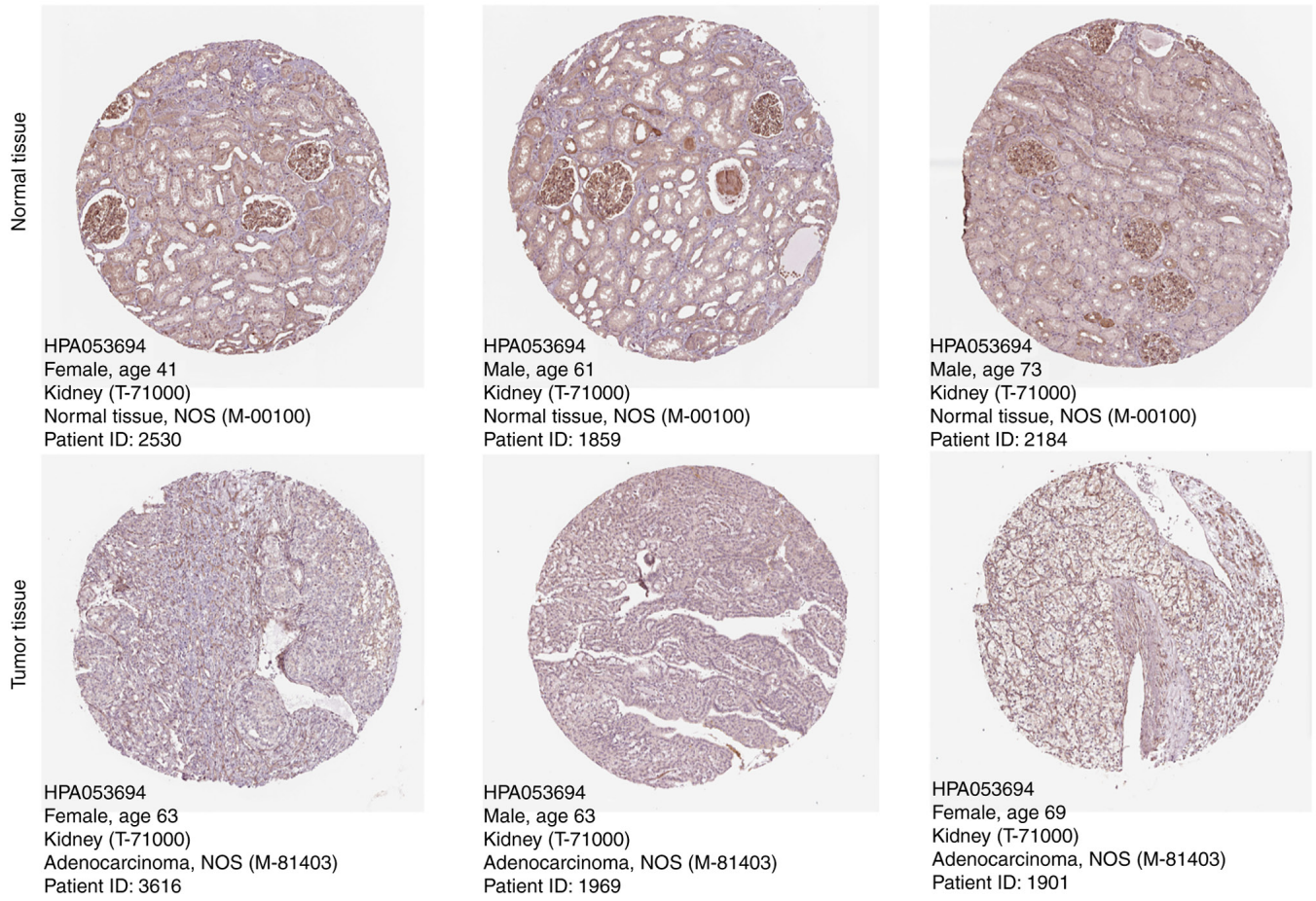

Figure 3. Immunohistochemical analysis data of thioredoxin-interacting protein expression in normal kidney and kidney renal clear cell carcinoma tissue from the Human Protein Atlas database. Magnification, x100. NOS, not otherwise specified.

with *TXNIP* mRNA expression (Fig. 5A-F). Furthermore, Kaplan-Meier analysis demonstrated that a high expression of these five genes was significantly associated with a good prognosis, compared with a low expression (Fig. 5G-K).

GO analysis results demonstrated that the function of *TXNIP* was mainly enriched in the 'acute-phase response', 'anatomical structure maturation' and 'acute-inflammatory response'. It was also associated with 'endopeptidase activity' and 'serine-type endopeptidase activity' (Fig. 5L). Moreover, the KEGG analysis showed there was a high association between the mRNA expression level of *TXNIP* and 'neuroactive ligand-receptor interactions' (Fig. 5M). KEGG genomic analyses demonstrated that five signaling pathways, including chemokine and T-cell receptor signaling pathways, were markedly differentially enriched at high mRNA expression levels of *TXNIP* (Fig. 5N). This finding suggests that *TXNIP* and its co-expressed genes have some association with the immune response of the organism.

Relationship between mRNA expression of TXNIP and KIRC immune cell infiltration. Fig. 6A demonstrates the distribution of the 21 tumor-infiltrating immune cells (TIICs) in the TCGA-KIRC dataset samples. Additionally, a comparative analysis of the *TXNIP* high and low expression groups was performed to assess the proportion of TIICs in the two groups. The results showed that seven TIICs differed significantly between the two groups (Fig. 6B). Among them, in the *TXNIP* high expression group, macrophages M1 (P=0.00045), dendritic cells resting (P=0.00028), monocytes (P=0.0014), macrophages M2 (P=0.0076), neutrophils (P=0.008), T cells CD4 memory resting (P<0.001) and mast cells resting (P<0.001) had significantly increased levels of infiltration, compared with that in the low expression group. In the *TXNIP* low expression group, the infiltration levels of macrophages M0 (P<0.001), T cells regulatory (Tregs; P<0.001) and T cells follicular helper (P<0.001) were significantly increased, compared with that in the high expression group. Furthermore, correlation analysis demonstrated that macrophages M1, mast cells resting, T cells CD4 memory resting and dendritic cells resting showed a significant positive association with *TXNIP* expression, and T cells follicular helper, Tregs and macrophages M0 exhibited a strong negative association with *TXNIP* expression (Fig. 6C-I). Fig. 6J not only reaffirms the high association of *TXNIP* mRNA expression levels with the immune cells aforementioned, but also visualizes the positive and negative association between various types of immune cells and *TXNIP* expression. These results indicated that *TXNIP* was a key player that regulated the immunological microenvironment of KIRC.

Correlation analysis of immune checkpoints. Following correlation analysis of the expression levels of immune checkpoint genes and *TXNIP* expression, 34 immune checkpoint-related

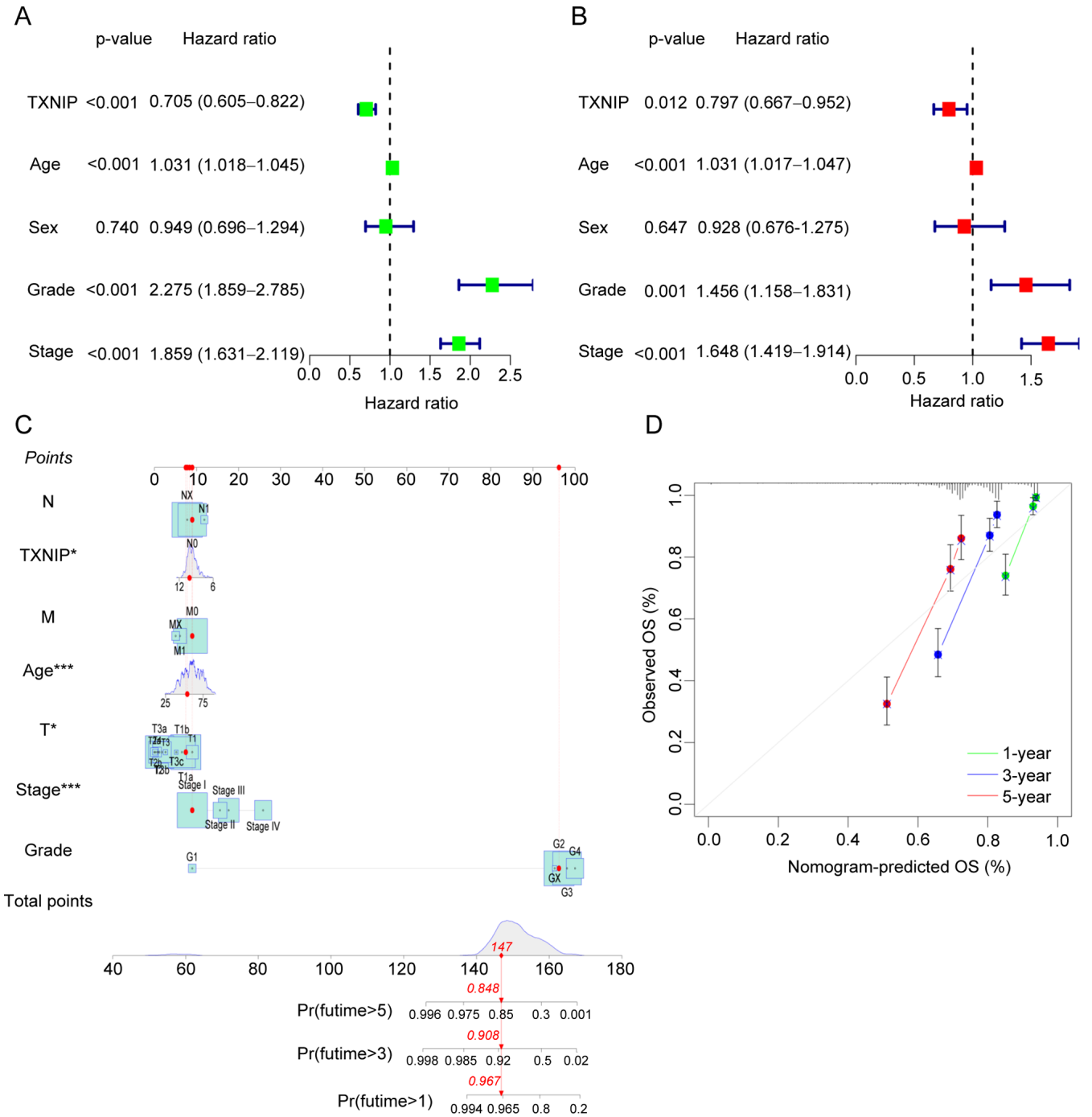

Figure 4. Univariate and multivariate Cox regression analysis of the prognostic value of *TXNIP* in KIRC. (A) Univariate Cox regression analysis and (B) Multivariate Cox regression analysis of *TXNIP* in KIRC. (C) Nomogram for predicting KIRC 1-year, 3-year and 5-year survival. (D) Calibration curves of the KIRC 1-year, 3-year and 5-year model. *P<0.05 and ***P<0.001. TXNIP, thioredoxin-interacting protein; KIRC, kidney renal clear cell carcinoma; OS, overall survival; N, node; M, metastasis; T, tumor; Pr, partial response.

genes were found to be strongly associated with the mRNA expression levels of *TXNIP*. With the exception of tumor necrosis factor superfamily member 14, a positive correlation between the mRNA expression levels of *TXNIP* and almost all the immune checkpoint genes was demonstrated. neuropilin 1, programmed cell death 1 ligand 2, CD200 and CD274 had the most notable positive associations with *TXNIP* expression of those genes assessed (Fig. 7A and B). The aforementioned results suggest that *TXNIP* is closely associated with the expression of most immune checkpoint-related genes.

TXNIP-specific expression in conventional CD4⁺ T cells (CD4Tconv). The association between *TXNIP* mRNA expression and several immune cells was assessed using the TISCH public database. The results demonstrated that *TXNIP* was mainly expressed in CD4Tconv cells (Fig. 8A and B). In addition, it was demonstrated that *TXNIP* was predominantly expressed in immune cells and stromal cells in KIRC (Fig. 8C). The aforementioned results suggest that *TXNIP* is associated with CD4⁺ T cells to a greater extent than other immune cells.

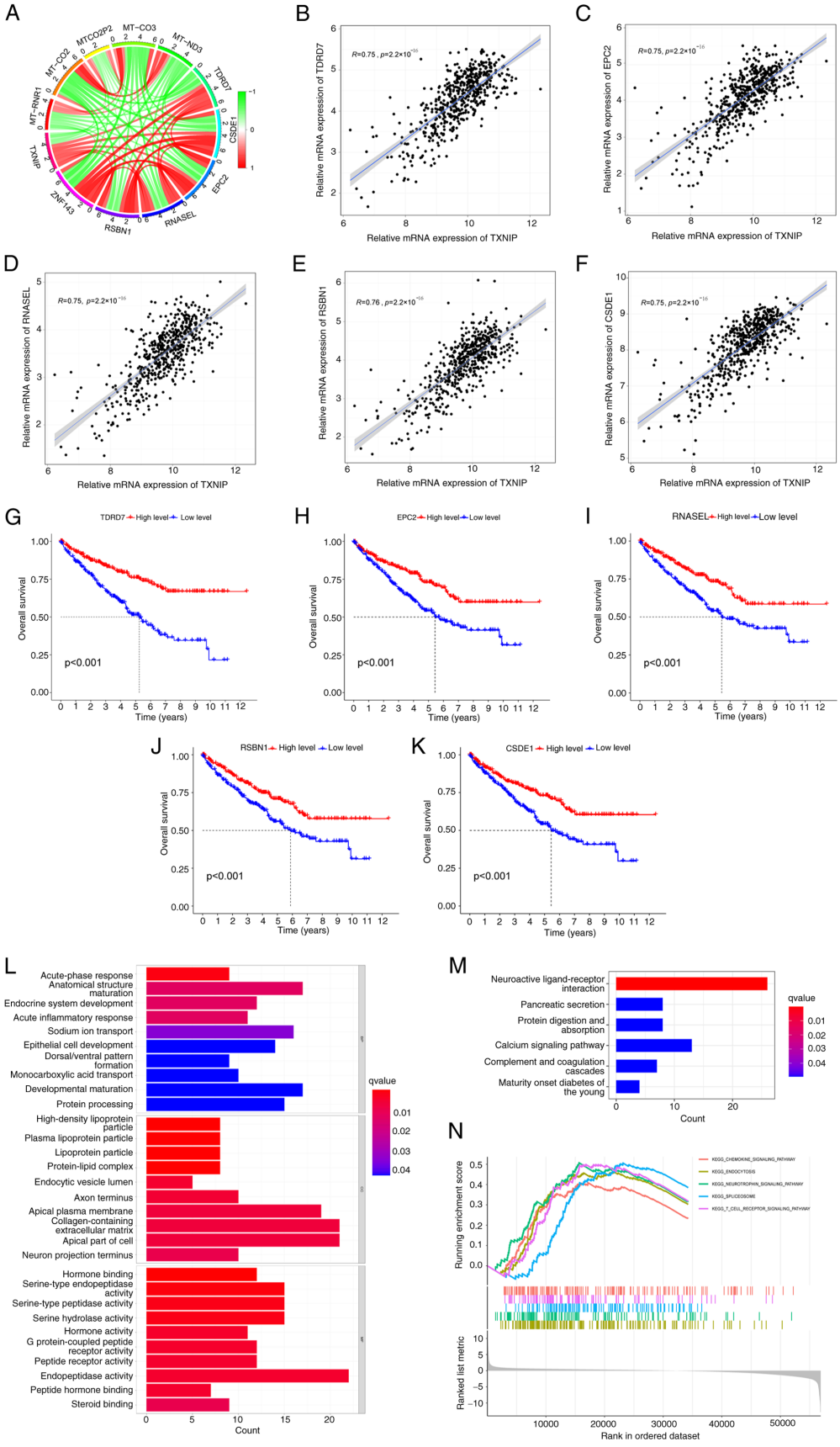

Figure 5. Identification and functional enrichment analysis of co-expressed genes. (A) Degree of association between 11 genes with a strong correlation with *TXNIP* (gene-gene associations are connected by shading, with red representing the degree of positive correlation and green representing the degree of negative correlation). Correlation between *TXNIP* and (B) TDRD7, (C) EPC2, (D) RNASEL, (E) RSBN1 and (F) CSDE1. Kaplan-Meier curves of the five co-expressed genes: (G) TDRD7, (H) EPC2, (I) RNASEL, (J) RSBN1 and (K) CSDE1. (L) Results of Gene Ontology enrichment analysis of co-expressed genes. (M) Results of Kyoto Encyclopedia of Genes and Genomes enrichment analysis of co-expressed genes (q-value is the optimized P-value). (N) The gene set enrichment analysis results show the five selected representative pathways. TXNIP, thioredoxin-interacting protein; TDRD7, tudor domain containing 7; CSDE1, cold shock domain containing E1; EPC2, enhancer of polycomb homolog 2; RSBN1, round spermatid basic protein 1; RNASEL, ribonuclease L.

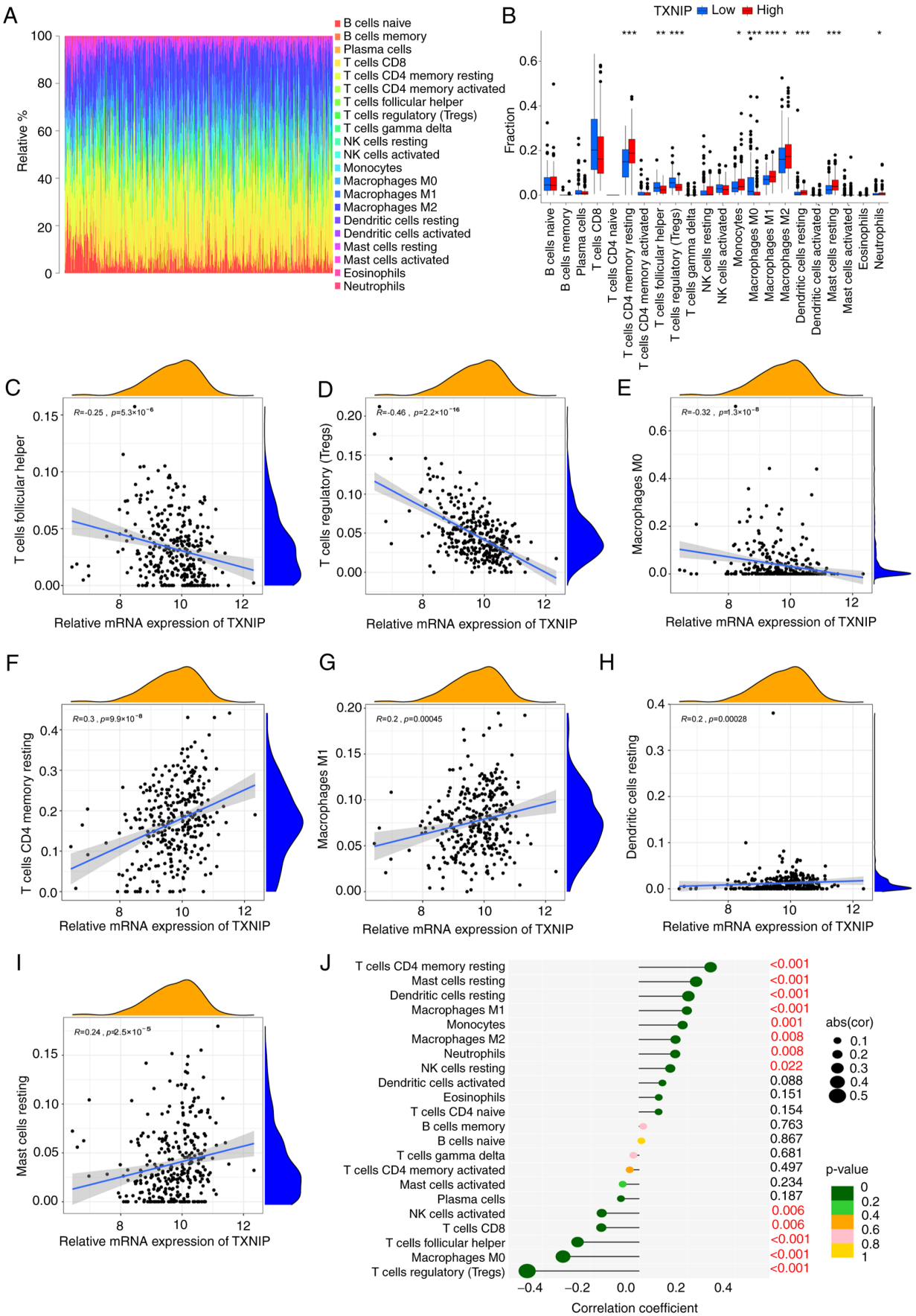

Figure 6. Relationship between *TXNIP* expression and immune cell infiltration in KIRC. (A) Characteristics of 21 tumor-infiltrating immune cells in the TCGA-KIRC samples. (B) Differences in immune infiltrating cells between high and low *TXNIP* expression subgroups. Correlation between *TXNIP* expression (C) T cells follicular helper, (D) T cells regulatory, (E) Macrophages M0, (F) T cells CD4 memory resting, (G) Macrophages M1, (H) Dendritic cells resting and (I) mast cells resting. (J) Correlation of *TXNIP* expression with 21 immune cells. *P<0.05, **P<0.01 and ***P<0.001. TXNIP, thioredoxin-interacting protein; KIRC, kidney renal clear cell carcinoma; Abs, absolute value; Cor, correlation coefficient.

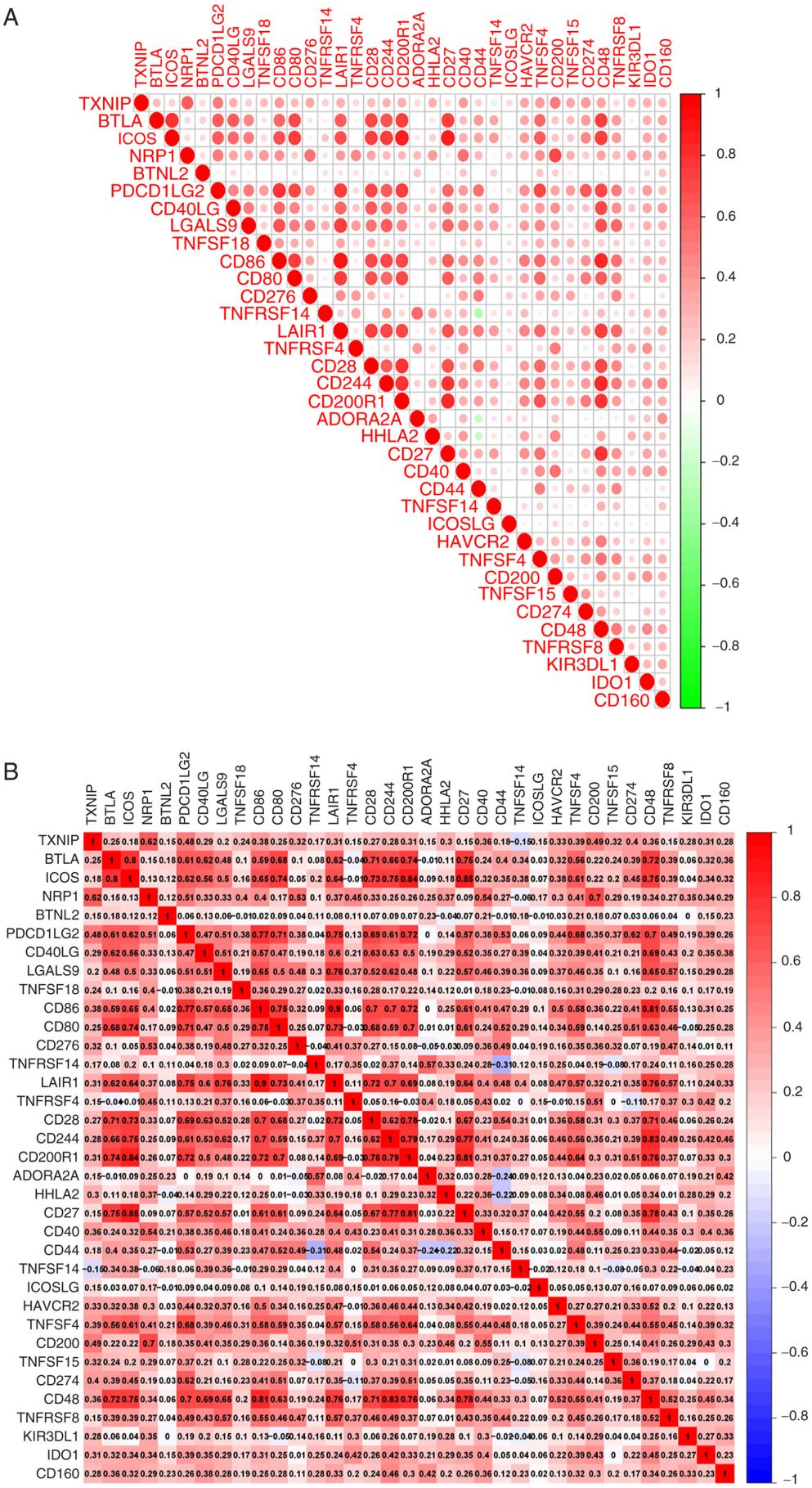

Figure 7. Correlation analysis of *TXNIP* expression in KIRC with immune checkpoints. (A) Degree of correlation between immune checkpoints and *TXNIP* expression. (B) Detailed demonstration of the correlation between different immune checkpoints. TXNIP, thioredoxin-interacting protein; KIRC, kidney renal clear cell carcinoma.

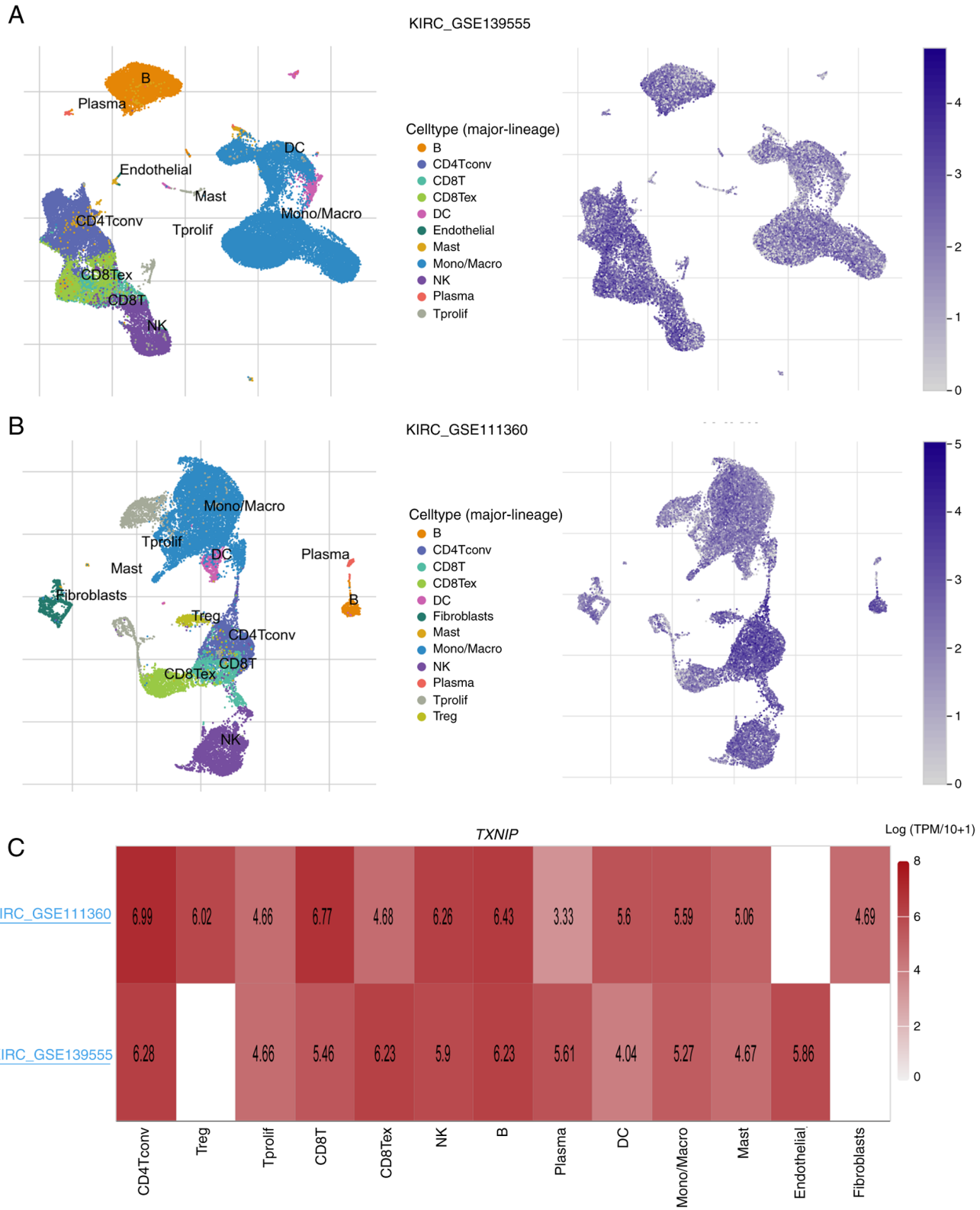

Figure 8. Characterization of *TXNIP* expression in different immune cells of KIRC. UMAP graphs presenting the distribution of immune cell populations (left) and their degree of association with *TXNIP* (right) analyzed through the (A) KIRC-GSE139555 and (B) KIRC-GSE111360 datasets using the TISCH database. (C) Degree of relationship between *TXNIP* expression and immune cells in different data sets. TXNIP, thioredoxin-interacting protein; KIRC, kidney renal clear cell carcinoma; TPM, transcipts per million; CD4Tconv, CD4T conventional lymphocytes; Treg, regulatory T cells; Tprolif, proliferating T cells; CD8Tex, exhausted CD8T cells; NK, natural killer cells; B, blymphocytes; Mono/Macro, monocytes/macrophages.

Drug sensitivity analysis of TXNIP. The CellMiner TM database was used to analyze whether there was a correlation between *TXNIP* expression and drug sensitivity. A total of 12 drugs were screened from 46 drugs, which were found to be significantly associated with the mRNA expression level of *TXNIP*, and the drug sensitivity was significantly enhanced in

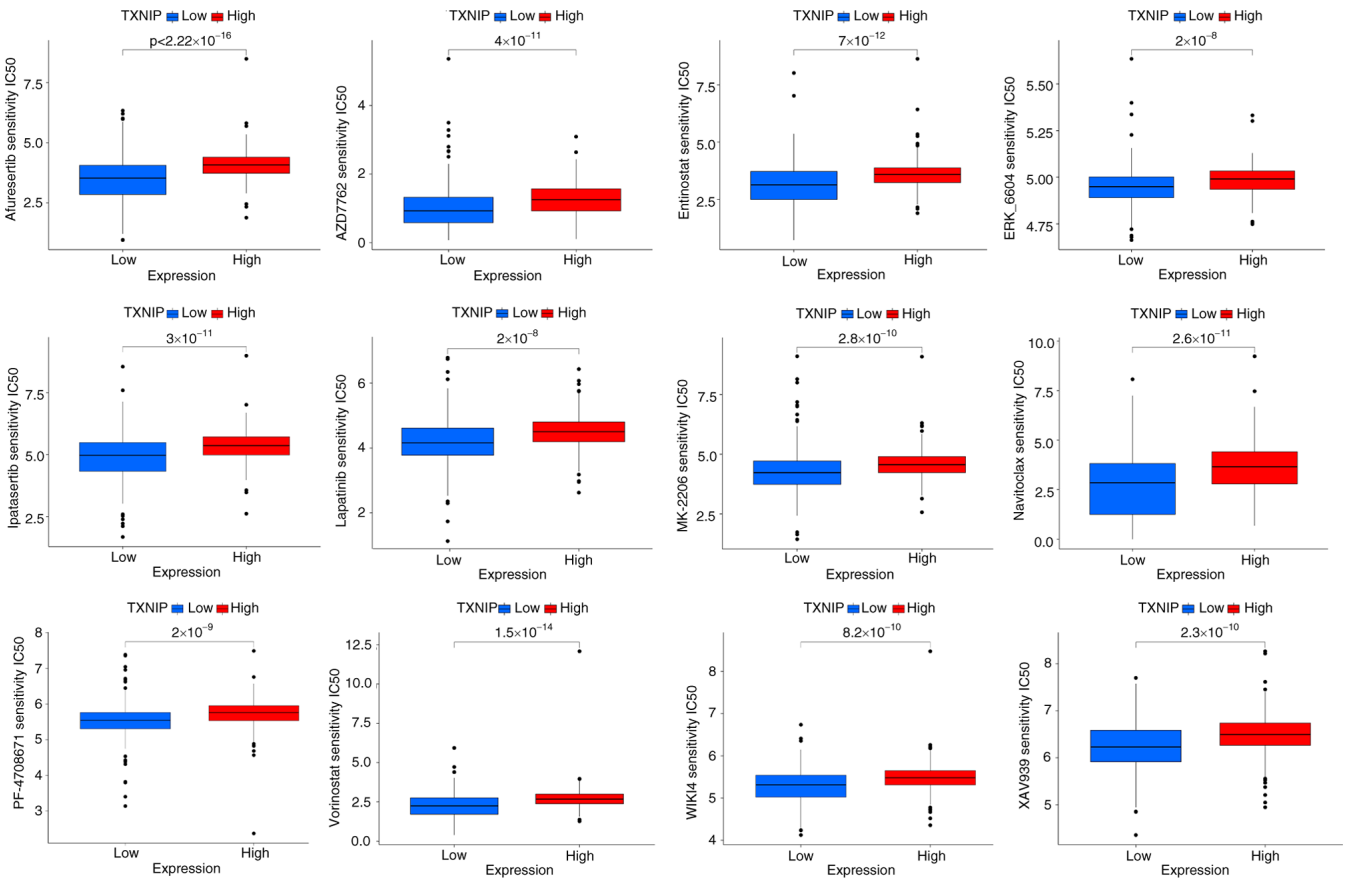

Figure 9. Drug sensitivity analysis of *TXNIP* expression in kidney renal clear cell carcinoma. TXNIP, thioredoxin-interacting protein.

the group with high *TXNIP* expression compared to the group with low *TXNIP* expression (Fig. 9). Among these, afuresertib, ipatasertib and MK-2206 are AKT kinase inhibitors (41), entinostat and vorinostat are histone deacetylase (HDAC) inhibitors (42,43), and WIKI4 and XAV939 are tankyrase inhibitors and have inhibitory effects on the Wnt/β-catenin signaling pathway (44,45). Therefore, we hypothesized that the increased expression of *TXNIP* may have some effect on the presence of the AKT, HDAC, tankyrase and Wnt/β-catenin signaling pathways compared to the generally low expression of *TXNIP* in cancer.

Cellular experimental validation. *TXNIP* expression levels in HK-2 and A498 cells differed substantially. The mRNA and protein expression levels of *TXNIP* in A498 cells were significantly lower than those in HK-2 cells, and these levels were significantly increased following the overexpression of *TXNIP*, compared with that in the A498-LV-Empty cells (Fig. 10A-C). Furthermore, the mRNA levels of CD25 and CTLA4, which are surface markers of $CD4^+$ T cells (46), were significantly reduced after the overexpression of *TXNIP*, compared with that in the A498-LV-Empty cells (Fig. 10C). Additionally, results from the CCK-8 assay showed that *TXNIP* overexpression significantly reduced the capacity of A498 cells to proliferate (Fig. 10D). These findings indicate that *TXNIP* acts as an important oncogene in KIRC, exerting inhibitory effects on immune escape and the rapid proliferation of cancer cells.

Discussion

KIRC is a heterogeneous disease with a poor prognosis (47). The limited predictors to assess the risk of KIRC may result in inaccurate grading, lowering the survival rate of patients with KIRC (48). Hence, the identification of reliable biomarkers for the prognosis and treatment of KIRC is urgently required. In the present study, high-throughput RNA sequencing data from the TCGA database was used and was further validated using RT-qPCR and western blot analyses. The findings revealed that *TXNIP* expression was significantly associated with OS, DSS and PFS, as well as the infiltration levels of TIICs. These findings highlight the potential for the use of *TXNIP* as a prognostic biomarker and therapeutic target for KIRC.

The primary structure of *TXNIP* includes an inhibitor-like N-terminus (10-152 aa) and a C-terminus (175-298 aa), indicating its role in the inhibition of the function of binding proteins (49-51). *TXNIP* is a recognized oncogene repressor in several types of breast cancer (52,53). Moreover, *TXNIP* expression has been reported to be significantly downregulated in breast, liver and lung cancers (54-56). In the present study, the expression of *TXNIP* in 33 tumor types was demonstrated, and it was compared with that of normal tissues using data from online databases. The results revealed that *TXNIP* was significantly downregulated in most cancers (Fig. 1B). Furthermore, RT-qPCR and western blotting demonstrated that *TXNIP* expression was significantly reduced in KIRC.

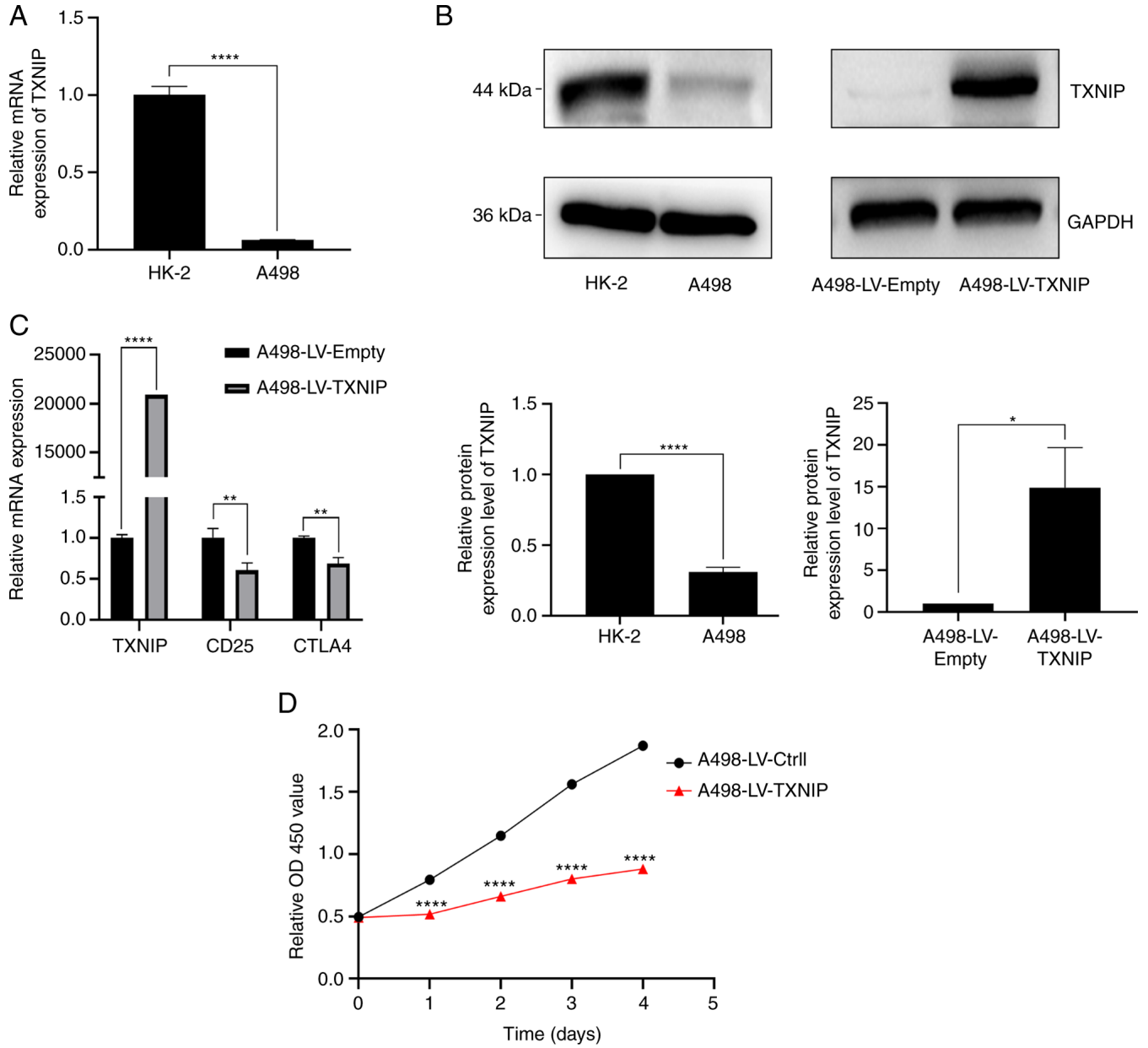

Figure 10. Cellular assay validation in KIRC. (A) Differences in *TXNIP* mRNA expression levels in HK-2 and A498 cells, assessed using RT-qPCR. (B) Differences in protein expression levels of TXNIP in HK-2 and A498 cells, and its protein expression changes in A498 after overexpression of *TXNIP*, assessed using western blotting. (C) mRNA expression changes of CD25 and CTLA4, the surface markers of $CD4^+$ T cells, after overexpression of *TXNIP*, assessed using RT-qPCR. (D) Effect of overexpression of *TXNIP* on the proliferation of kidney cancer A498 cells, assessed using the Cell Counting Kit-8 assay. *P<0.05; **P<0.01; ****P<0.0001. TXNIP, thioredoxin-interacting protein; KIRC, kidney renal clear cell carcinoma; RT-qPCR, reverse transcription-quantitative PCR; CTLA4, cytotoxic T-lymphocyte-associated protein 4; OD, optical density.

The significance of *TXNIP* as a prognostic factor has been demonstrated in patients with cancer. In hepatocellular carcinoma, lower *TXNIP* expression was notably associated with a worse prognosis (55). *TXNIP* was also identified as an independent prognostic factor for distant metastasis-free survival and OS in gastroesophageal adenocarcinoma (57) and the prognostic and predictive value of *TXNIP* have been established in human breast cancer (58,59). The present study found that reduced mRNA expression of *TXNIP* was associated with unfavorable clinicopathological features, including high histological grade, stage and the occurrence of distant metastases (Fig. 2E-I). Multivariate Cox regression analysis demonstrated that *TXNIP* was an independent prognostic factor that significantly impacted PFS, DSS and OS. Reduced *TXNIP* expression was also associated with adverse clinical outcomes in KIRC. Furthermore, the analyses, stratified by sex, age, TNM stage, stage and grade, demonstrated that patients with high mRNA expression levels of *TXNIP* expression experienced significantly greater OS in comparison with those patients with low levels of expression. The findings by Gao *et al* (32) similarly showed that reduced *TXNIP* mRNA expression was significantly associated with clinical stage. In addition, the study also showed that *TXNIP* was an independent prognostic factor for KIRC by univariate and multivariate Cox analysis (32). In contrast to this study, the present study not only used TCGA, the TIMER and HPA databases and

related experiments (Fig. 10A and B) for further assessment to ensure the reliability of the results, but also screened for co-expressed genes and performed Kaplan-Meier analyses on the co-expressed genes (Fig. 5G-K) to evaluate their association with prognosis.

In the tumor microenvironment, the ecosystem established by TIICs serves a crucial role in the regulation of cancer progression in KIRC, and the immune responses are a critical determinant of survival outcomes. Hence, the proportion of TIICs in cancer potentially has prognostic value (60-62). Further analysis using TCGA and CIBERSORT revealed that certain immune cells associated with *TXNIP* expression were significantly associated with the survival of patients with KIRC. Increased *TXNIP* mRNA expression was associated with an increase in macrophages M1, T cells CD4 memory resting, mast cells resting and dendritic cells resting. Conversely, there was a decrease in the proportion of T cells follicular helper, Tregs and macrophages M0 (Fig. 6B). The ability of the chemokine signaling pathway to control T cell migration toward chemokine sources has been demonstrated. In the context of cancer, ligands for C-C chemokine receptor type 5 and CXC motif chemokine receptor 3 have also been reported to be associated with the degree of tumor-infiltrating lymphocyte (TIL) infiltration in cancer (63-65). Reactive oxygen species (ROS) metabolism is controlled by the essential component *TXNIP* and cytosolic ROS in $CD4^+$ T lymphocytes rapidly decrease during the contraction phase. Once $CD4^+$ T cells activation is attenuated, *TXNIP* has been reported to be quickly upregulated, and furthermore, *TXNIP* expression has also been directly associated with the development of allergen-specific memory Th2 cells (66). Results from the present study demonstrated that the T-cell receptor and chemokine pathways were notably differentially enriched in KIRC with high *TXNIP* mRNA expression, according to the gene set enrichment analysis data (Fig. 5N). Additionally, the outcomes of RT-qPCR assays revealed that *TXNIP* mRNA expression was significantly associated with $CD4^+$ T cells in KIRC (Fig. 10C). These findings demonstrate that *TXNIP* regulates immune infiltration and may affect the levels of ROS in patients with KIRC.

Additionally, the present study found a significant association between the mRNA levels of *TXNIP* and sensitivity to 12 antitumor drugs (Fig. 9). WIKI4 and XAV-939 are known to suppress tankyrase activity, inhibiting Wnt/β-catenin signaling pathway-mediated transcription (44,45). Afuresertib, ipatasertib and MK-2206 are key antitumor drugs as they potentially inhibit AKT kinase (41). Elevated levels of *TXNIP* expression can suppress the activity of the Wnt/β-catenin and PI3K/AKT/mTOR signaling pathways (67-69). This mechanism may therefore be related to enhanced drug sensitivity, but further evaluation is needed.

Whilst the present study offers insights on the potential function of *TXNIP* on KIRC prognosis and immune infiltration, certain limitations merit attention. Primarily, the sample size was only 614 cases and a larger data set is needed to confirm the accuracy of the findings. Additionally, further experimental studies are needed to confirm the functional role of *TXNIP* in KIRC.

In summary, the present study indicated that there is a strong association between decreased *TXNIP* expression levels, insufficient immune cell infiltration and poor prognosis in patients with KIRC, and that the reduction in *TXNIP* expression levels may impair the antitumor activity of the immune system in patients with KIRC. These findings provide insights that may prove beneficial in the development of novel immunotherapeutic approaches.

Acknowledgements

Not applicable.

Funding

Funding was received from the Guangxi Zhuang Autonomous Region Health and Family Planning Commission (grant. no. Z-L20221837).

Availability of data and materials

The datasets used and/or analyzed during the current study are available from the corresponding author on reasonable request. The data accessed in the present study may be found in the TCGA (https://portal.gdc.cancer.gov/), HPA (http://www.proteinatls.org), and TIMER (https://cistrome.shinyapps.io/timer/) databases.

Authors' contributions

WL, ZX and MD contributed to the development of the statistical analysis strategies to collect, evaluate and organize data from the databases; design, implementation and processing of experimental data; analysis of data; and drafting and revision of the manuscript. XL and ZH designed and directed the study, provided experimental design ideas, guidance on data processing and advice on manuscript revision. WL and ZX wrote the main manuscript text and prepared Figs. 1-4. MD prepared Fig. 5-10. All authors have read and approved the final manuscript. WL and ZX confirm the authenticity of all the raw data.

Ethics approval and consent to participate

Not applicable.

Patient consent for publication

Not applicable.

Competing interests

The authors declare that they have no competing interests.

References

1. Siegel RL, Miller KD and Jemal A: Cancer statistics, 2019. CA Cancer J Clin 69: 7-34, 2019.
2. Shuch B, Amin A, Armstrong AJ, Eble JN, Ficarra V, Lopez-Beltran A, Martignoni G, Rini BI and Kutikov A: Understanding pathologic variants of renal cell carcinoma: Distilling therapeutic opportunities from biologic complexity. Eur Urol 67: 85-97, 2015.
3. Sonpavde G, Choueiri TK, Escudier B, Ficarra V, Hutson TE, Mulders PF, Patard JJ, Rini BI, Staehler M, Sternberg CN and Stief CG: Sequencing of agents for metastatic renal cell carcinoma: Can we customize therapy? Eur Urol 61: 307-316, 2012.

4. Bella L, Zona S, Nestal de Moraes G and Lam EW: Foxm1: A key oncofoetal transcription factor in health and disease. Semin Cancer Biol 29: 32-39, 2014.
5. Mitchell TJ, Turajlic S, Rowan A, Nicol D, Farmery JHR, O'Brien T, Martincorena I, Tarpey P, Angelopoulos N, Yates LR, *et al*: Timing the landmark events in the evolution of clear cell renal cell cancer: Tracerx Renal. Cell 173: 611-623.e17, 2018.
6. Bedke J, Gauler T, Grünwald V, Hegele A, Herrmann E, Hinz S, Janssen J, Schmitz S, Schostak M, Tesch H, *et al*: Systemic therapy in metastatic renal cell carcinoma. World J Urol 35: 179-188, 2017.
7. Chatterjee N and Bivona TG: Polytherapy and targeted cancer drug resistance. Trends Cancer 5: 170-182, 2019.
8. Noessner E, Brech D, Mendler AN, Masouris I, Schlenker R and Prinz PU: Intratumoral alterations of dendritic-cell differentiation and CD8(+) T-cell anergy are immune escape mechanisms of clear cell renal cell carcinoma. Oncoimmunology 1: 1451-1453, 2012.
9. Choueiri TK, Fishman MN, Escudier B, McDermott DF, Drake CG, Kluger H, Stadler WM, Perez-Gracia JL, McNeel DG, Curti B, *et al*: Immunomodulatory activity of nivolumab in metastatic renal cell carcinoma. Clin Cancer Res 22: 5461-5471, 2016.
10. Lalani AA, McGregor BA, Albiges L, Choueiri TK, Motzer R, Powles T, Wood C and Bex A: Systemic treatment of metastatic clear cell renal cell carcinoma in 2018: Current paradigms, use of immunotherapy, and future directions. Eur Urol 75: 100-110, 2019.
11. Carlo MI, Voss MH and Motzer RJ: Checkpoint inhibitors and other novel immunotherapies for advanced renal cell carcinoma. Nat Rev Urol 13: 420-431, 2016.
12. Gill DM and Agarwal N: Cancer immunotherapy: A paradigm shift in the treatment of advanced urologic cancers. Urol Oncol 35: 676-677, 2017.
13. Martínez-Salamanca JI, Huang WC, Millán I, Bertini R, Bianco FJ, Carballido JA, Ciancio G, Hernández C, Herranz F, Haferkamp A, *et al*: Prognostic impact of the 2009 UICC/AJCC TNM staging system for renal cell carcinoma with venous extension. Eur Urol 59: 120-127, 2011.
14. Brahmer JR, Drake CG, Wollner I, Powderly JD, Picus J, Sharfman WH, Stankevich E, Pons A, Salay TM, McMiller TL, *et al*: Phase I study of single-agent anti-programmed death-1 (MDX-1106) in refractory solid tumors: Safety, clinical activity, pharmacodynamics, and immunologic correlates. J Clin Oncol 28: 3167-3175, 2010.
15. Lipson EJ, Sharfman WH, Drake CG, Wollner I, Taube JM, Anders RA, Xu H, Yao S, Pons A, Chen L, *et al*: Durable cancer regression off-treatment and effective reinduction therapy with an anti-PD-1 antibody. Clin Cancer Res 19: 462-468, 2013.
16. Topalian SL, Hodi FS, Brahmer JR, Gettinger SN, Smith DC, McDermott DF, Powderly JD, Carvajal RD, Sosman JA, Atkins MB, *et al*: Safety, activity, and immune correlates of anti-PD-1 antibody in cancer. N Engl J Med 366: 2443-2454, 2012.
17. Motzer RJ, Rini BI, McDermott DF, Redman BG, Kuzel TM, Harrison MR, Vaishampayan UN, Drabkin HA, George S, Logan TF, *et al*: Nivolumab for metastatic renal cell carcinoma: Results of a randomized phase ii trial. J Clin Oncol 33: 1430-1437, 2015.
18. Motzer RJ, Escudier B, McDermott DF, George S, Hammers HJ, Srinivas S, Tykodi SS, Sosman JA, Procopio G, Plimack ER, *et al*: Nivolumab versus everolimus in advanced renal-cell carcinoma. N Engl J Med 373: 1803-1813, 2015.
19. Brahmer JR, Tykodi SS, Chow LQ, Hwu WJ, Topalian SL, Hwu P, Drake CG, Camacho LH, Kauh J, Odunsi K, *et al*: Safety and activity of anti-PD-L1 antibody in patients with advanced cancer. N Engl J Med 366: 2455-2465, 2012.
20. McDermott DF, Sosman JA, Sznol M, Massard C, Gordon MS, Hamid O, Powderly JD, Infante JR, Fassò M, Wang YV, *et al*: Atezolizumab, an anti-programmed death-ligand 1 antibody, in metastatic renal cell carcinoma: Long-term safety, clinical activity, and immune correlates from a phase Ia study. J Clin Oncol 34: 833-842, 2016.
21. Yang JC, Hughes M, Kammula U, Royal R, Sherry RM, Topalian SL, Suri KB, Levy C, Allen T, Mavroukakis S, *et al*: Ipilimumab (anti-CTLA4 antibody) causes regression of metastatic renal cell cancer associated with enteritis and hypophysitis. J Immunother 30: 825-830, 2007.
22. Sharpe AH and Pauken KE: The diverse functions of the PD1 inhibitory pathway. Nat Rev Immunol 18: 153-167, 2018.
23. Chen KS and DeLuca HF: Isolation and characterization of a novel cDNA from HL-60 cells treated with 1,25-dihydroxyvitamin D-3. Biochim Biophys Acta 1219: 26-32, 1994.
24. Wu N, Zheng B, Shaywitz A, Dagon Y, Tower C, Bellinger G, Shen CH, Wen J, Asara J, McGraw TE, *et al*: Ampk-dependent degradation of TXNIP upon energy stress leads to enhanced glucose uptake via GLUT1. Mol Cell 49: 1167-1175, 2013.
25. Shen L, O'Shea JM, Kaadige MR, Cunha S, Wilde BR, Cohen AL, Welm AL and Ayer DE: Metabolic reprogramming in triple-negative breast cancer through Myc suppression of TXNIP. Proc Natl Acad Sci USA 112: 5425-5430, 2015.
26. Han SH, Jeon JH, Ju HR, Jung U, Kim KY, Yoo HS, Lee YH, Song KS, Hwang HM, Na YS, *et al*: Vdup1 upregulated by TGF-beta1 and 1,25-dihydorxyvitamin d3 inhibits tumor cell growth by blocking cell-cycle progression. Oncogene 22: 4035-4046, 2003.
27. Saxena G, Chen J and Shalev A: Intracellular shuttling and mitochondrial function of thioredoxin-interacting protein. J Biol Chem 285: 3997-4005, 2010.
28. Zhou R, Yazdi AS, Menu P and Tschopp J: A role for mitochondria in NLRP3 inflammasome activation. Nature 469: 221-225, 2011.
29. Zhou R, Tardivel A, Thorens B, Choi I and Tschopp J: Thioredoxin-interacting protein links oxidative stress to inflammasome activation. Nat Immunol 11: 136-140, 2010.
30. Jiao D, Huan Y, Zheng J, Wei M, Zheng G, Han D, Wu J, Xi W, Wei F, Yang AG, *et al*: UHRF1 promotes renal cell carcinoma progression through epigenetic regulation of TXNIP. Oncogene 38: 5686-5699, 2019.
31. Meszaros M, Yusenko M, Domonkos L, Peterfi L, Kovacs G and Banyai D: Expression of TXNIP is associated with angiogenesis and postoperative relapse of conventional renal cell carcinoma. Sci Rep 11: 17200, 2021.
32. Gao Y, Qi JC, Li X, Sun JP, Ji H and Li QH: Decreased expression of TXNIP predicts poor prognosis in patients with clear cell renal cell carcinoma. Oncol Lett 19: 763-770, 2020.
33. Pan M, Zhang F, Qu K, Liu C and Zhang J: TXNIP: A double-edged sword in disease and therapeutic outlook. Oxid Med Cell Longev 2022: 7805115, 2022.
34. Hutter C and Zenklusen JC: The cancer genome atlas: Creating lasting value beyond its data. Cell 173: 283-285, 2018.
35. Subramanian A, Tamayo P, Mootha VK, Mukherjee S, Ebert BL, Gillette MA, Paulovich A, Pomeroy SL, Golub TR, Lander ES and Mesirov JP: Gene set enrichment analysis: A knowledge-based approach for interpreting genome-wide expression profiles. Proc Natl Acad Sci USA 102: 15545-15550, 2005.
36. Yu G, Wang LG, Han Y and He QY: clusterProfiler: An R package for comparing biological themes among gene clusters. OMICS 16: 284-287, 2012.
37. Chen B, Khodadoust MS, Liu CL, Newman AM and Alizadeh AA: Profiling tumor infiltrating immune cells with CIBERSORT. Methods Mol Biol 1711: 243-259, 2018.
38. Li B, Severson E, Pignon JC, Zhao H, Li T, Novak J, Jiang P, Shen H, Aster JC, Rodig S, *et al*: Comprehensive analyses of tumor immunity: Implications for cancer immunotherapy. Genome Biol 17: 174, 2016.
39. Shankavaram UT, Varma S, Kane D, Sunshine M, Chary KK, Reinhold WC, Pommier Y and Weinstein JN: CellMiner: A relational database and query tool for the NCI-60 cancer cell lines. BMC Genomics 10: 277, 2009.
40. Livak KJ and Schmittgen TD: Analysis of relative gene expression data using real-time quantitative PCR and the 2(-Delta Delta C(T)) method. Methods 25: 402-408, 2001.
41. Wu JH, Limmer AL, Narayanan D, Doan HQ, Simonette RA, Rady PL and Tyring SK: The novel AKT inhibitor afuresertib suppresses human Merkel cell carcinoma MKL-1 cell growth. Clin Exp Dermatol 46: 1551-1554, 2021.
42. Trapani D, Esposito A, Criscitiello C, Mazzarella L, Locatelli M, Minchella I, Minucci S and Curigliano G: Entinostat for the treatment of breast cancer. Expert Opin Investig Drugs 26: 965-971, 2017.
43. Athira KV, Sadanandan P and Chakravarty S: Repurposing Vorinostat for the treatment of disorders affecting brain. Neuromolecular Med 23: 449-465, 2021.
44. James RG, Davidson KC, Bosch KA, Biechele TL, Robin NC, Taylor RJ, Major MB, Camp ND, Fowler K, Martins TJ and Moon RT: WIKI4, a novel inhibitor of tankyrase and wnt/ß-catenin signaling. PLoS One 7: e50457, 2012.
45. Yu J, Liu D, Sun X, Yang K, Yao J, Cheng C, Wang C and Zheng J: CDX2 inhibits the proliferation and tumor formation of colon cancer cells by suppressing Wnt/β-catenin signaling via transactivation of GSK-3β and Axin2 expression. Cell Death Dis 10: 26, 2019.

46. Haddadi MH and Negahdari B: Clinical and diagnostic potential of regulatory T cell markers: From bench to bedside. Transplant Immunol 70: 101518, 2022.
47. Wang L, Zhu Y, Ren Z, Sun W, Wang Z, Zi T, Li H, Zhao Y, Qin X, Gao D, *et al*: An immunogenic cell death-related classification predicts prognosis and response to immunotherapy in kidney renal clear cell carcinoma. Front Oncol 13: 1147805, 2023.
48. Sun Z, Tao W, Guo X, Jing C, Zhang M, Wang Z, Kong F, Suo N, Jiang S and Wang H: Construction of a Lactate-related prognostic signature for predicting prognosis, tumor microenvironment, and immune response in kidney renal clear cell carcinoma. Front Immunol 13: 818984, 2022.
49. Zhou J, Yu Q and Chng WJ: TXNIP (VDUP-1, TBP-2): A major redox regulator commonly suppressed in cancer by epigenetic mechanisms. Int J Biochem Cell Biol 43: 1668-1673, 2011.
50. Patwari P, Higgins LJ, Chutkow WA, Yoshioka J and Lee RT: The interaction of thioredoxin with Txnip. Evidence for formation of a mixed disulfide by disulfide exchange. J Biol Chem 281: 21884-21891, 2006.
51. Zhang P, Wang C, Gao K, Wang D, Mao J, An J, Xu C, Wu D, Yu H, Liu JO and Yu L: The ubiquitin ligase itch regulates apoptosis by targeting thioredoxin-interacting protein for ubiquitin-dependent degradation. J Biol Chem 285: 8869-8879, 2010.
52. Iqbal MA, Chattopadhyay S, Siddiqui FA, Ur Rehman A, Siddiqui S, Prakasam G, Khan A, Sultana S and Bamezai RN: Silibinin induces metabolic crisis in triple-negative breast cancer cells by modulating EGFR-MYC-TXNIP axis: Potential therapeutic implications. FEBS J 288: 471-485, 2021.
53. Chen D, Dang BL, Huang JZ, Chen M, Wu D, Xu ML, Li R and Yan GR: Mir-373 drives the epithelial-to-mesenchymal transition and metastasis via the mir-373-TXNIP-HIF1α-TWIST signaling axis in breast cancer. Oncotarget 6: 32701-32712, 2015.
54. Cadenas C, Franckenstein D, Schmidt M, Gehrmann M, Hermes M, Geppert B, Schormann W, Maccoux LJ, Schug M, Schumann A, *et al*: Role of thioredoxin reductase 1 and thioredoxin interacting protein in prognosis of breast cancer. Breast Cancer Res 12: R44, 2010.
55. Hamilton JP, Potter JJ, Koganti L, Meltzer SJ and Mezey E: Effects of vitamin D3 stimulation of thioredoxin-interacting protein in hepatocellular carcinoma. Hepatol Res 44: 1357-1366, 2014.
56. Hong SY, Yu FX, Luo Y and Hagen T: Oncogenic activation of the PI3K/AKT pathway promotes cellular glucose uptake by downregulating the expression of thioredoxin-interacting protein. Cell Signal 28: 377-383, 2016.
57. Woolston CM, Madhusudan S, Soomro IN, Lobo DN, Reece-Smith AM, Parsons SL and Martin SG: Thioredoxin interacting protein and its association with clinical outcome in gastro-oesophageal adenocarcinoma. Redox Biol 1: 285-291, 2013.
58. Yang MH, Wu MZ, Chiou SH, Chen PM, Chang SY, Liu CJ, Teng SC and Wu KJ: Direct regulation of TWIST by HIF-1alpha promotes metastasis. Nat Cell Biol 10: 295-305, 2008.
59. Sheth SS, Bodnar JS, Ghazalpour A, Thipphavong CK, Tsutsumi S, Tward AD, Demant P, Kodama T, Aburatani H and Lusis AJ: Hepatocellular carcinoma in Txnip-deficient mice. Oncogene 25: 3528-3536, 2006.
60. Grivennikov SI, Greten FR and Karin M: Immunity, inflammation, and cancer. Cell 140: 883-899, 2010.
61. Picard E, Verschoor CP, Ma GW and Pawelec G: Relationships between immune landscapes, genetic subtypes and responses to immunotherapy in colorectal cancer. Front Immunol 11: 369, 2020.
62. Wang SS, Liu W, Ly D, Xu H, Qu L and Zhang L: Tumor-infiltrating B cells: Their role and application in anti-tumor immunity in lung cancer. Cell Mol Immunol 16: 6-18, 2019.
63. Ribas A and Wolchok JD: Cancer immunotherapy using checkpoint blockade. Science 359: 1350-1355, 2018.
64. Denkert C, von Minckwitz G, Brase JC, Sinn BV, Gade S, Kronenwett R, Pfitzner BM, Salat C, Loi S, Schmitt WD, *et al*: Tumor-infiltrating lymphocytes and response to neoadjuvant chemotherapy with or without carboplatin in human epidermal growth factor receptor 2-positive and triple-negative primary breast cancers. J Clin Oncol 33: 983-991, 2015.
65. Ding Q, Lu P, Xia Y, Ding S, Fan Y, Li X, Han P, Liu J, Tian D and Liu M: CXCL9: Evidence and contradictions for its role in tumor progression. Cancer Med 5: 3246-3259, 2016.
66. Kokubo K, Hirahara K, Kiuchi M, Tsuji K, Shimada Y, Sonobe Y, Shinmi R, Hishiya T, Iwamura C, Onodera A and Nakayama T: Thioredoxin-interacting protein is essential for memory T cell formation via the regulation of the redox metabolism. Proc Natl Acad Sci USA 120: e2218345120, 2023.
67. Zhu J and Han S: Histone deacetylase 10 exerts anti-tumor effects on cervical cancer via a novel microRNA-223/TXNIP/Wnt/β-catenin pathway. IUBMB Life: Jan 22, 2021 (Epub ahead of print). doi: 10.1002/iub.2448.
68. Dong F, Dong S, Liang Y, Wang K, Qin Y and Zhao X: Mir-20b inhibits the senescence of human umbilical vein endothelial cells through regulating the Wnt/β-catenin pathway via the TXNIP/NLRP3 axis. Int J Mol Med 45: 847-857, 2020.
69. Ao H, Li H, Zhao X, Liu B and Lu L: TXNIP positively regulates the autophagy and apoptosis in the rat müller cell of diabetic retinopathy. Life Sci 267: 118988, 2021.

Copyright © 2024 Liu et al. This work is licensed under a Creative Commons Attribution-NonCommercial-NoDerivatives 4.0 International (CC BY-NC-ND 4.0) License.